Biology of Reproduction, 2023, 1–14
https://doi.org/10.1093/biolre/ioad004
Research Article

OXFORD

Effects of a ketogenic diet on reproductive and metabolic phenotypes in mice with polycystic ovary syndrome†

Shihe Liu[1,‡], Qiyang Yao[1,‡], Xiaolian Li[2], Haowen Wu[1], Changwei Sun[1], Wenpei Bai[2,*] and Jihong Kang[1,*]

[1]Department of Physiology and Pathophysiology, School of Basic Medical Sciences, Peking University Health Science Center, Beijing, China
[2]Department of Obstetrics and Gynecology, Beijing Shijitan Hospital Affiliated to Capital Medical University, Beijing, China

***Correspondence:** Jihong Kang, PhD, Department of Physiology and Pathophysiology, School of Basic Medical Sciences, Peking University Health Science Center, No.38 Xueyuan Rd, Haidian, Beijing 100191, China. Tel: 86-10-82805613; E-mail: kangjihong@bjmu.edu.cn; Wenpei Bai, MD, PhD, Department of Obstetrics and Gynecology, Beijing Shijitan Hospital Affiliated to Capital Medical University, Beijing 100038, China. Tel: 86-10-63926260; E-mail: baiwp@bjsjth.cn

†**Grant Support:** This work was supported by the National Natural Science Foundation of China (82171634, 31971068, and 81670733).

‡Contributed equally to this work.

Abstract

Polycystic ovary syndrome (PCOS) is one of the most common female reproductive and metabolic disorders. The ketogenic diet (KD) is a diet high in fat and low in carbohydrate. The beneficial effects of KD intervention have been demonstrated in obese women with PCOS. The underlying mechanisms, however, remain unknown. The aim of the present study was to investigate the effects of a KD on both reproductive and metabolic phenotypes of dehydroepiandrosterone (DHEA)-induced PCOS mice. Female C57BL/6 mice were divided into three groups, designated Control, DHEA, and DHEA+KD groups. Mice of both Control and DHEA groups were fed the control diet, whereas DHEA+KD mice were fed a KD with 89%(kcal) fat for 1 or 3 weeks after PCOS mouse model was completed. At the end of the experiment, both reproductive and metabolic characteristics were assessed. Our data show that KD treatment significantly increased blood ketone levels, reduced body weight and random and fasting blood glucose levels in DHEA+KD mice compared with DHEA mice. Glucose tolerance, however, was impaired in DHEA+KD mice. Ovarian functions were improved in some DHEAmice after KD feeding, especially in mice treated with KD for 3 weeks. In addition, inflammation and cell apoptosis were inhibited in the ovaries of DHEA+KD mice. Results from in vitro experiments showed that the main ketone body β-hydroxybutyrate reduced inflammation and cell apoptosis in DHEA-treated KGN cells. These findings support the therapeutic effects of KD and reveal a possible mechanism by which KD improves ovarian functions in PCOS mice.

Summary Sentence Our findings support the role of KD intervention in weight loss, reducing blood glucose, and improving ovarian functions in PCOS mice and reveal a possible mechanism by which KD improved ovarian functions by inhibiting inflammation and cell apoptosis in ovarian granulosa cells in PCOS.

Keywords: polycystic ovary syndrome, the ketogenic diet, reproductive phenotypes, metabolic phenotypes

Introduction

Polycystic ovary syndrome (PCOS) is one of the most common endocrine disorders, affecting 5–10% of the women of reproductive age [1]. It is characterized by hyperandrogenism, menstrual dysfunction, polycystic ovaries, anovulatory infertility, hirsutism, and acne [2, 3]. PCOS also involves metabolic abnormalities, including obesity, dyslipidemia, and insulin resistance (IR) [4]. It is thus now considered as an important metabolic disorder as well as reproductive morbidity [5]. Oral contraceptives, anti-androgen therapy, metformin, etc., are common treatments for women with PCOS. For patients who are overweight or obese, lifestyle interventions, such as weight loss and exercise, remain the most basic means of regulating menses, preventing progression to type 2 diabetes mellitus (T2DM) and lowering cardiovascular risk [6].

The ketogenic diet (KD) is a high-fat and low-carbohydrate diet that was developed as a treatment for epilepsy [7]. KD treatment shifts the body toward fat metabolism [8] and aims to mimic the metabolic profile of fasting by reducing blood glucose concentration and increasing blood ketone concentration [7]. In addition to epilepsy, researches on KD have received rapid attention over the past decade. Evidence of the promising therapeutic potential of the KD has emerged in the treatment of other diseases, including obesity, T2DM, nonalcoholic fatty liver disease, and PCOS [6]. In a pilot study, women with PCOS and a body mass index over 27 kg/m^2 showed a significant reduction in body weight, free testosterone, and fasting insulin after the KD treatment for 6 months [9]. Recently, Li et al. [3] also reported the beneficial effects of KD on improving the menstrual cycle and liver function, suggesting that KD may be considered as a valuable nonpharmacological treatment for obese women with PCOS and liver dysfunction.

Although KD treatment seems promising in patients with PCOS and obesity, the underlying mechanisms still remain unclear. In the present study, we thus investigated the effects of a KD on both reproductive and metabolic phenotypes in a dehydroepiandrosterone (DHEA)-induced PCOS mouse model. Meanwhile, the possible mechanisms were studied.

Materials and method

Animals and experimental protocols

Female C57BL/6 J mice were (21 days of age) purchased from the animal facility of the Peking University Health Science Center. The mice were maintained in a standard laboratory

Received: May 13, 2022. **Revised:** November 11, 2022. **Accepted:** January 19, 2023

condition with a 12-h light/dark cycle at 22 ± 2 °C with free access to rodent feed and water. At postnatal day 25, the mice of comparable body weights were randomly divided into three groups ($n = 12$ per group). Group 1: Control group. The mice were fed a normal chow and injected subcutaneously daily with sesame oil (0.1-ml/100-g body weight). Group 2: DHEA group. Mice were fed a normal chow and injected subcutaneously daily with DHEA (6-mg/100-g body weight) dissolved in 0.1 ml of sesame oil. Group 3: DHEA+KD group. Mice were fed a normal chow and injected subcutaneously daily with DHEA (6-mg/100-g body weight) dissolved in 0.1 ml of sesame oil. After 20 days of the treatments, the mice of Control group were fed a control diet (10% of calories from fat; 10% of calories from protein; 80% of calories from carbohydrate, Biopike, China) and injected subcutaneously daily with sesame oil for 1 or 3 weeks. Mice of DHEA group were fed a control diet and injected subcutaneously daily with DHEA for 1 or 3 weeks. Mice of DHEA+KD group were fed a KD (89.9% of calories from fat; 10% of calories from protein; 0.1% of calories from carbohydrate, Biopike, China) and injected subcutaneously daily with DHEA for 1 or 3 weeks. During the treatment, the mice were weighed daily. The body weight gain of the mice was calculated by subtracting the body weight after KD treatment from the body weight before KD treatment. In addition, energy intake of the mice was recorded every day. The amount of energy intake of the DHEA+KD mice was strictly controlled according to the amount of enery intake of DHEA mice the day before and did not exceed energy intake of the DHEA mice. After the treatments for 1 or 3 weeks, both reproductive and metabolic features were evaluated. DHEA and sesame oil were purchased from Sigma-Aldrich (St-Louis, MO, USA). All animal experiments were approved by the Animal Care and Use Review Committee of Peking University Health Science Center accordance with the Guide for the Care and Use of Laboratory Animals published by the US National Institutes of Health.

Estrous cycle determination

The estrous cycle ($n = 6$ per group) was determined daily 11 days after the treatments (Day 56 of life) (treatments for 3 weeks) and assessed for 10 consecutive days, or 1 day after the treatment (Day 46 of life) (treatments for 1 week) and assessed for 7 consecutive days. Vaginal cells were collected via saline lavage, fixed and then stained with methylene blue (0.1%). The stages of the estrous cycle were determined based on vaginal cytology: predominant leukocytes indicated the diestrus stage, predominant nucleated epithelial cells indicated the proestrus stage, predominant cornified squamous epithelial cells indicated the estrus stage, and both cornified squamous epithelial cells and leukocytes indicated the metaestrus stage.

Oral glucose tolerance test

Oral glucose tolerance test (OGTT) was performed 3 days before the end of the treatments ($n = 6$ per group). Mice were fasted for 12 h before administration of glucose (3-g/kg body weight per 3 ml) by oral gavage. Blood samples were collected from the tail vein for the measurements of blood glucose levels immediately before glucose administration and then at 15, 30, 60, 90, and 120 min with the OneTouch Ultra glucometer (Accu-Check Sensor; Roche Diagnostics). Data were presented as the absolute values of blood glucose concentrations. Total area under the curve (AUC) of the glucose response was calculated using GraphPad Prism 8.0 software.

Insulin tolerance test

The mice were fasted for 4 h before an insulin tolerance test (ITT) and blood glucose was measured before insulin administration ($n = 6$ per group). Then, the mice were injected intraperitoneally with insulin (1-IU/kg body weight). Then, blood samples were collected from the tail vein and blood glucose was measured immediately at 15, 30, 60, 90, and 120 min after injection. Data were presented as the absolute values of blood glucose concentrations. Total AUC of the glucose values was calculated using GraphPad Prism 8.0 software.

Blood ketone measurement

Blood ketone levels were measured 1 day before the end of the treatments ($n = 6$ per group). Blood samples were collected from the tail vein for the measurements of blood ketone levels immediately with the blood ketone monitoring system (FreeStyle Optium Neo, Abbott).

Indirect calorimetry measurement

Indirect calorimetry was performed before the mice were killed ($n = 6$ per group). Indirect calorimetry was performed as described previously [10]. In brief, the mice were individually housed in metabolic cages (Oxylet, PanLab, Spain) for 24 h to acclimate to the conditions and then monitored for a 24-h period to measure Oxygen consumption (VO_2) and Carbon deoxidate production (VCO_2). Spontaneous activities of the mice were monitored by activity sensor at the same time. The respiratory quotient ($RQ = VCO_2/VO_2$) and energy expenditure (EE) (in kcal/-day/kg $0.75 = [3.815 + 1.232 \times RQ] \times VO_2 \times 1.44$) were calculated using Metabolism software (Oxylet, PanLab, Spain).

Tissue collection and histology

The animals were anesthetized via an intraperitoneal injection of a mixture of ketamine hydrochloride (100 mg/kg) and xylazine (20 mg/kg). Blood samples were collected from angular vein. The parametrial and perirenal fat of the mice were dissected and collected as intra-abdominal fat samples and weighed. Ovary samples were then rapidly removed from the animals. One ovary of each mouse was fixed in 4% paraformaldehyde (PFA) and post-fixed in 20% sucrose solution. Then, the ovaries were embedded in paraffin and cut into sections (6-μm thickness). Ovary sections were stained with hematoxylin and eosin (H&E) according to the standard histological procedures. To examine ovarian morphology, every 12th section was mounted on a glass slide. Numbers of corpora lutea and cystic follicles were counted ($n = 6$ per group). Another ovary of each mouse was snap frozen in liquid nitrogen and then kept at −80 °C for RNA extraction.

Measurement of serum sex steroids

Serum testosterone levels ($n = 6$ per group) were determined with ^{125}I-labeled radioimmunoassay kits (Beijing North Institute of Biological Technology). The within-assay and between-assay variabilities were 10 and 15%, respectively.

Cell culture and treatments

KGN cells, a human ovarian granulosa cell line, were purchased from Beijing Aitemeng Science and Technology

Table 1. Primer sequences used for real-time PCR.

Gene name	source	Primer sequences		Product length (bp)
β-actin	Mouse	Sence	5'-TGAGCTGCGTTTTACACCCT-3'	198
		Antisence	5'-GCCTTCACCGTTCCAGTTTT-3'	
β-actin	Human	Sence	5'-CTTCGCGGGCGACGAT-3'	103
		Antisence	5'-CACATAGGAATCCTTCTGACCCAT-3'	
IL-1β	Mouse	Sence	5'-TGCCACCTTTTGACAGTGATG-3'	138
		Antisence	5'-TGATGTGCTGCTGCGAGATT-3'	
IL-1β	Human	Sence	5'-AGTACCTGAGCTCGCCAGT-3'	160
		Antisence	5'-GTGGTGGTCGGAGATTCGTAG-3'	
IL-6	Mouse	Sence	5'-GACAAAGCCAGAGTCCTTCAGA-3'	76
		Antisence	5'-TGTGACTCCAGCTTATCTCTTGG-3'	
IL-6	Human	Sence	5'-ACAAGCGCCTTCGGTCCAGTT-3'	142
		Antisence	5'-TTCGTTCTGAAGAGGTGAGTGGCT-3'	

Co (catalog number: BNCC-337610). Cells were cultured in Dulbecco's Modified Eagle's Medium (DMEM) containing 4500-mg/l glucose and supplemented with 10% fetal bovine serum (FBS) (TIANHANG Bio-Technology and Science Inc.) and 100-U/ml penicillin/streptomycin in a humidified 5% CO_2 atmosphere at 37 °C. The medium was changed every 2 days. At confluence, KGN cells were pretreated with different concentrations of BHB (0, 1, 5, 10, and 15 mM) for 6 h and then were treated with different concentrations of BHB plus DHEA (5×10^{-5} M) in triplicate for 24 h at 37 °C in an atmosphere of 5% CO_2:95% air. After the treatments, the cells were collected for protein assay and other experiments.

Culture of mouse primary granulosa cells

The mouse primary granulosa cells (mGCs) were collected and cultured as reported with some modifications [11]. In brief, female C57BL/6 mice (age 21 days) were intraperitoneally injected with pregnant mare serum gonadotropin (PMSG) (10 IU) to induce ovulation. Then, the mice were killed by cervical dislocation. The ovaries were quickly removed and put into a 10-cm cell culture dish containing PBS. The granulosa cells were isolated using needle puncture methods and then centrifuged at 800 rpm for 5 min. The supernatant was discarded, and the cell pellets were washed with Dulbecco's Modified Eagle's Medium, F12 (DMEM/F12) (GIBCO, USA) and then cultured into 6-well plates in DMEM/F12 supplemented with 10% FBS (HyClone, USA) and 100 U/ml penicillin/streptomycin in a humidified 5% CO_2 atmosphere at 37 °C.

Flow cytometry

Primary mGCs were plated into six-well plates. After confluence, cells were treated with DHEA (0, 5×10^{-5} M) or DHEA plus BHB (BHB (0, 1, 5, and 10 mM) for 24 h as KGN cells. Then, the cells were gently digested with 0.5% trypsin (EDTA-free) and rinsed with PBS twice. Subsequently, the cells were fixed with 4% paraformaldehyde for 10 min at 4 °C and then permeabilized in 0.3% Triton-X (Sigma-Aldrich, USA). Cells were blocked in 5% bovine serum albumin for 10 min at 4 °C and then incubated with rabbit monoclonal antibody against cleaved Caspase-3 (Cell singaling Technology, USA) at a dilution of 1:200. Fluorescence was obtained by reation with a fluorescent secondary antibody (Alexa Fluor 488 goat anti-rabbit secondary antibody, ThermoFisher Scientific, USA) at a dilution of 1:500 for 10 min at 4 °C. Finally, the samples were subjected to flow cytometry (Guava easycyte 5, Millipore, USA). All data were analyzed using Flow.jo_V10.6.2 software.

Methyl tetrazolium assay

Cells were seeded in a 96-well tissue culture plate at a density of 1×10^4 cells/well. KGN cells were treated with different concentrations of BHB and DHEA (5×10^{-5} M) for 24 h. Cells treated with the vehicle served as the controls. After the treatments, Methyl tetrazolium (MTT) was added to each well and the cells were further incubated at 37 °C for 4 h. Dimethyl sulfoxide was added to each well after removing the medium. After shaking the plates for 5 min, the absorbance of the mixture was measured at 490 nm using a microplate enzyme-linked immunosorbent assay (ELISA) reader (Bio-Rad, USA).

Real- time PCR

Total RNA was extracted from the ovaries and cells by using TRIzol reagent (CWbio, China). Aliquots of 2 μg of total RNA from each sample were reverse transcribed to cDNA with a reverse transcription kit (Vazyme, China). Primer sequences (Table 1) were designed on NCBI website. Real-time PCR was performed using fluorescent SYBR Green PCR Master Mix (Vazyme, China) according to the manufacturer's instructions (Agilent Technologies, USA). β-actin was used as an internal control. The expression of the target genes was normalized to that of β-actin in the same sample using the $2^{-\Delta\Delta Ct}$ method. Each sample was measured in duplicate in each experiment.

Western blot analysis

Western blot analysis was performed as described previously [5]. Briefly, aliquots of 20 μg of protein from tissues or cells were separated by 8–12% SDS-PAGE and transferred to nitrocellulose membrane. The membrane was blocked in 5% skimmed milk for 1 h at room temperature and then incubated with primary antibodies at 4 °C overnight. The antibodies to Caspase-3 and Cleaved caspase-3 were purchased from Cell Signaling Technology. β-actin was used as an internal control. The antibody to β-actin was bought from Proteintech. The membrane was washed with TBST buffer and then incubated with a horseradish peroxide-conjugated secondary antibody at room temperature for 1 h. After washing, the membrane was developed with ECL Reagent (Yeasen, China) and the blots were visualized using chemiluminescent detection (Tanon 5200). Protein expression level was quantified with Image J software.

TUNEL staining

The apoptosis of the ovarian tissues from the mice was detected by terminal deoxynucleotidyl transferase-mediated

dUTP nick-end labeling (TUNEL) staining with a commercially available kit from Yeasen (TUNEL Apoptosis Detection Kit, Yeasen, China) according to the manufacturer's instructions ($n = 5$ per group).

UHPLC–MS/MS analysis

Serum samples were taken for nontargeted metabolomic analysis ($n = 8$ per group). Metabolomics profiling was analyzed using a UPLC-ESI-Q-TOF-MS (UHPLC, 1290 Infinity LC, Agilent Technologies, Santa Clara, CA) equipped with TripleTOF 5600 (AB Sciex, Framingham, MA). For hydrophilic interaction liquid chromatography separation, samples were analyzed using a ACQUIY UPLC BEH Amide (2.1 × 100 mm, 1.7 μm) column (Waters, Ireland). The mobile phase consisted of A (25-mM ammonium acetate and 25-mM ammonium hydroxide in water) and B (100% acetonitrile, ACN) with a flow rate of 0.5 ml/min. The MS system was operated in positive and negative electrospray ionization (ESI) mode. The source temperature was 600 °C. A high-sensitivity mode was selected for information-dependent acquisition during product ion scanning. The collisional energy was fixed at 30 V and declustering potential at 60 V.

For data normalization, quality control (QC) samples were prepared by pooling aliquots of all representative serum samples. Blank samples (75% ACN in water) and QC samples were injected every six samples during data acquisition.

Data pre-processing and filtering

The raw MS data were converted to MzXML files using ProteoWizard MSConvert and processed using XCMS for feature detection, retention time correction, and alignment. The metabolites were identified by accurate mass (<25 ppm) and MS/MS data which were matched with a standards database. In the extracted-ion features, variables showing over 50% of the nonzero measurement values in at least one group were included for further statistical analysis.

Multivariate statistical analysis

SIMCA-P software (Version 14.0, Umetrics, Umea, Sweden) was utilized for multivariate pattern recognition analysis and model establishment. The peak area in chromatograms were used for multivariate statistical analysis in current study. PCA was used in the model for the analyze of specimen separation and outliers. Subsequently, OPLS-DA and PLS-DA were both performed to displace variation between control and experimental groups. Evaluated models were calculated for over-fitting with methods of permutation tests. R2X and R2Y values were used to described the performance of the models, while Q2 and permutation test ($n = 200$) were performed to evaluate model prediction performance. The variable importance on projection (VIP) values more than 1.0 and P-values less than 0.05 were considered as statistically significant in this model. Fold change was derived from the logarithm of the average mass response (area) ratio between two arbitrary classes.

Statistical analysis

Data are presented as mean ± standard deviation (SD). Statistical analyses were performed with GraphPad Prism 8.0 software. Data for multiple comparisons were statistically analyzed by one-way ANOVA followed by Bonferroni post-test. $P<0.05$ was considered statistically significant.

Results

The KD reduced body weight of DHEA mice

Female C57BL/6 J mice at 25-day age were treated with sesame oil (control mice) or dehydroepiandrosterone (DHEA) for 20 days to induce prepubertal PCOS mouse model as described previously [5]. Then, the control mice were treated with a control diet (control group) and PCOS mice were treated with a control diet (DHEA group) or a KD (DHEA+KD group) for 1 or 3 weeks. As shown in Figure 1A and B, the energy intake of the control mice and DHEA was similar during the treatment for 1 or 3 weeks. The energy intake of the DHEA+KD mice was lower than the DHEA mice at the beginning of the feeding, and then was similar to that of DHEA animals. After the treatments, the final body weight and body weight gain of the DHEA+KD mice treated for 1 or 3 weeks were significantly decreased compared with the DHEA mice (Figure 1C–F). In addition, we also measured the weight of the intra-abdominal fat when tissues were collected. The intra-abdominal fat weight/body weight of the DHEA+KD mice were also markedly reduced in DHEA+KD mice treated for 1 or 3 weeks than DHEA mice (Figure 1G and H).

KD reduced blood glucose levels and increased ketone levels

To investigate the effects of the KD treatment on glucose metabolism in DHEA mice for 1 and 3 weeks, we measured the random blood glucose and fasting blood glucose levels. The results showed that both random blood glucose and fasting blood glucose levels in DHEA+KD mice treated with KD for 1 or 3 weeks were significantly reduced compared with DHEA mice (Figure 2A–D). Blood ketone levels of the mice were also measured. As expected, blood ketone levels were significantly higher in DHEA+KD mice treated for 1 or 3 weeks (Figure 2E and F), confirming the success of the KD treatment. There was no apparent difference in blood ketone levels between the control and DHEA animals.

KD improved insulin tolerance but impaired glucose tolerance of DHEA mice

To further investigate the effects of the KD on glucose tolerance and insulin sensitivity in DHEA mice, OGTT and ITT were performed in the three groups of mice. The DHEA+KD mice showed impaired glucose tolerance after the KD treatment for 1 or 3 weeks (Figure 3A and B). There was a trend of improvement, but no significant difference in insulin sensitivity in DHEA+KD mice treated for 3 weeks compared with DHEA mice (Figure 3C). In contrast, insulin sensitivity was greatly improved in DHEA+KD mice treated for 1 week compared with the DHEA mice (Figure 3D).

KD increased energy metabolism of DHEA mice

Indirect calorimetry was performed at the end of the experiment to determine RQ and EE of the animals. RQ values in both the light and dark periods were remarkably lower in the DHEA+KD mice treated for 1 or 3 weeks than in control and DHEA animals (Figure 4A and B). RQ mainly reflected the substrates utilized by energy metabolism of the body. The reduced RQ values in the DHEA+KD mice suggested the increased fat utilization in these animals. The average EE in DHEA mice was comparable to control mice, but the EE values were significantly higher in the DHEA+KD mice

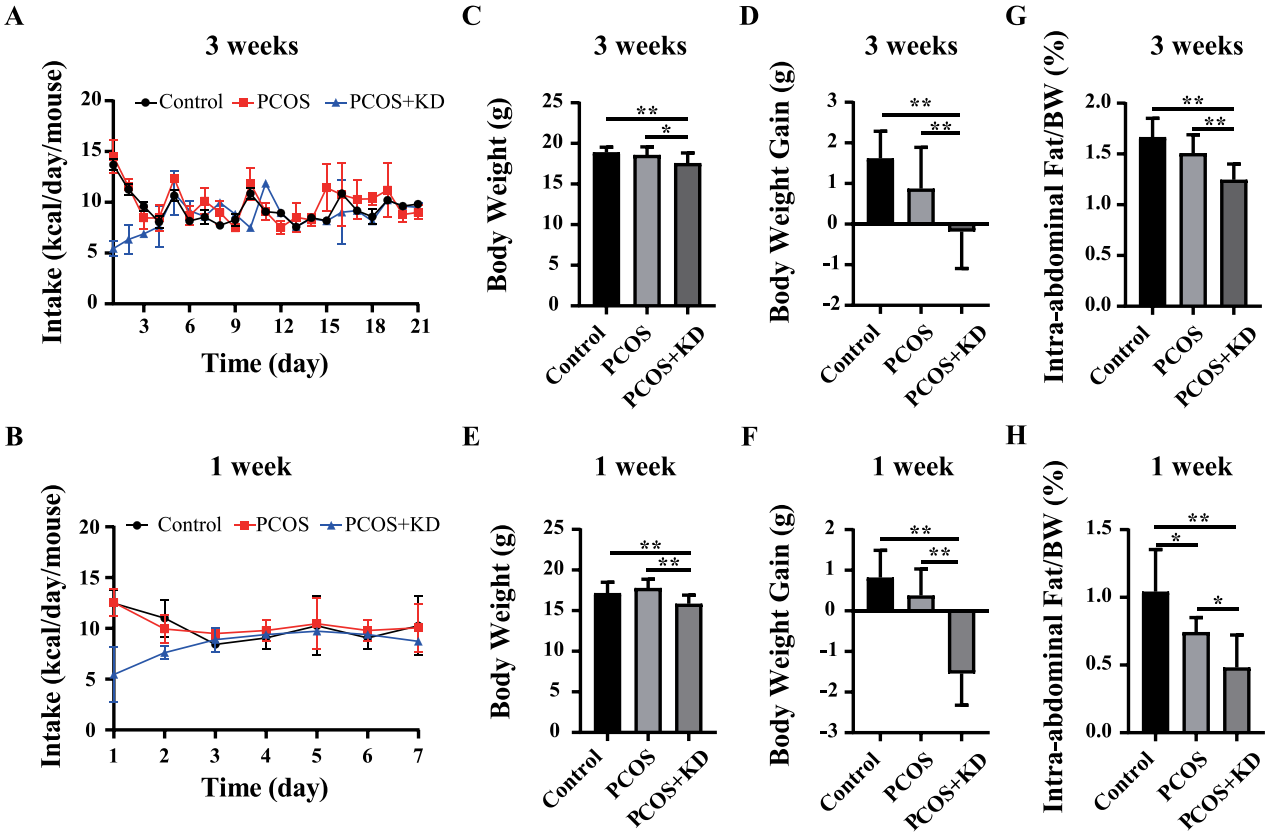

Figure 1. Effects of a KD feeding on food intake, body weight, and intra-abdominal fat mass. (A) Energy intake of mice for 3 weeks. (B) Energy intake of mice for 1 week. (C) Body weight of the mice treated a control diet or KD for 3 weeks. (D) Body weight gain of the mice treated a control diet or KD for 3 weeks (relative to the beginning of the diet treatment). (E) Body weight of the mice treated with a control diet or KD for 1 week. (F) Body weight gain of the mice treated with a control diet or KD for 1 week. (G) Intra-abdominal fat/body weight of the mice treated with a control diet or KD for 3 weeks. (H) Intra-abdominal fat/body weight of the mice treated with a control diet or KD for 1 week. Data are presented as mean ± SD. *, $P<0.05$, **, $P<0.01$, $n=12$ per group.

treated for 3 weeks than in the control mice (Figure 4C). There was no statistical difference between DHEA+KD and DHEA animals treated for 3 weeks. In contrast, no obvious difference was observed in the average EE among the three groups of mice treated for 1 week (Figure 4D). Meanwhile, the activity of these mice was monitored. The total activity of the mice during 24 h was significantly lower in the DHEA+KD mice treated for 1 or 3 weeks compared with the DHEA and control mice (Figure 4E and F), indicating that the increased EE in DHEA+KD mice treated for 3 weeks was not due to the increased activity of these animals.

KD treatment improved the ovarian function of DHEA mice

To investigate the effect of the KD on the reproductive phenotype of the DHEA mice, we first measured the serum testosterone levels of the animals. The serum testosterone levels of the DHEA mice and DHEA+KD mice were markedly higher than in the control animals treated for 1 or 3 weeks, whereas there was no apparent difference between DHEA+KD mice and DHEA mice (Figure 5A). These results suggested that androgen levels are not appreciably different between DHEA and DHEA+KD mice.

Menstrual disturbance is a typical clinical characteristic of women with PCOS. We therefore monitored the estrous cycles of mice for 10 days during the 3-week treatment and 7 days during the 1-week treatment, respectively. The data showed that control mice exhibited normal estrous cycles. In contrast, PCOS mice showed disrupted estrous cycles as reported previously [5] (Figure 5B). The estrous cycles of about 50% DHEA+KD mice treated for 3 weeks and 33% DHEA+KD mice treated for 1 week were normal (Figure 5B and Table 2), suggesting that the KD improved ovarian function of some DHEA mice.

H&E staining was performed with the ovary sections (Figure 5C) and the numbers of corpora lutea and cystic follicles were counted. As shown in Figure 5D and E, the number of corpora lutea was significantly lower and the number of ovarian cystic follicles was significantly higher in the DHEA mice than in control mice. After treatment with KD for 1 or 3 weeks, there was a trend in an increase in the number of corpora lutea and a reduction in the number of ovarian cystic follicles in DHEA+KD mice compared with DHEA mice (Figure 5D and E). However, there was no statistical difference in the number of corpora lutea or the number of ovarian cystic follicles between DHEA+KD mice and DHEA mice. These data suggested that the KD only improved ovarian function in individuals of the DHEA mice but not all of them.

KD treatment changed serum metabolites of DHEA mice

Since the KD treatment for 3 weeks seemed to improve the reproductive phenotype of DHEA mice better than the KD treatment for 1 week, we then performed nontargeted

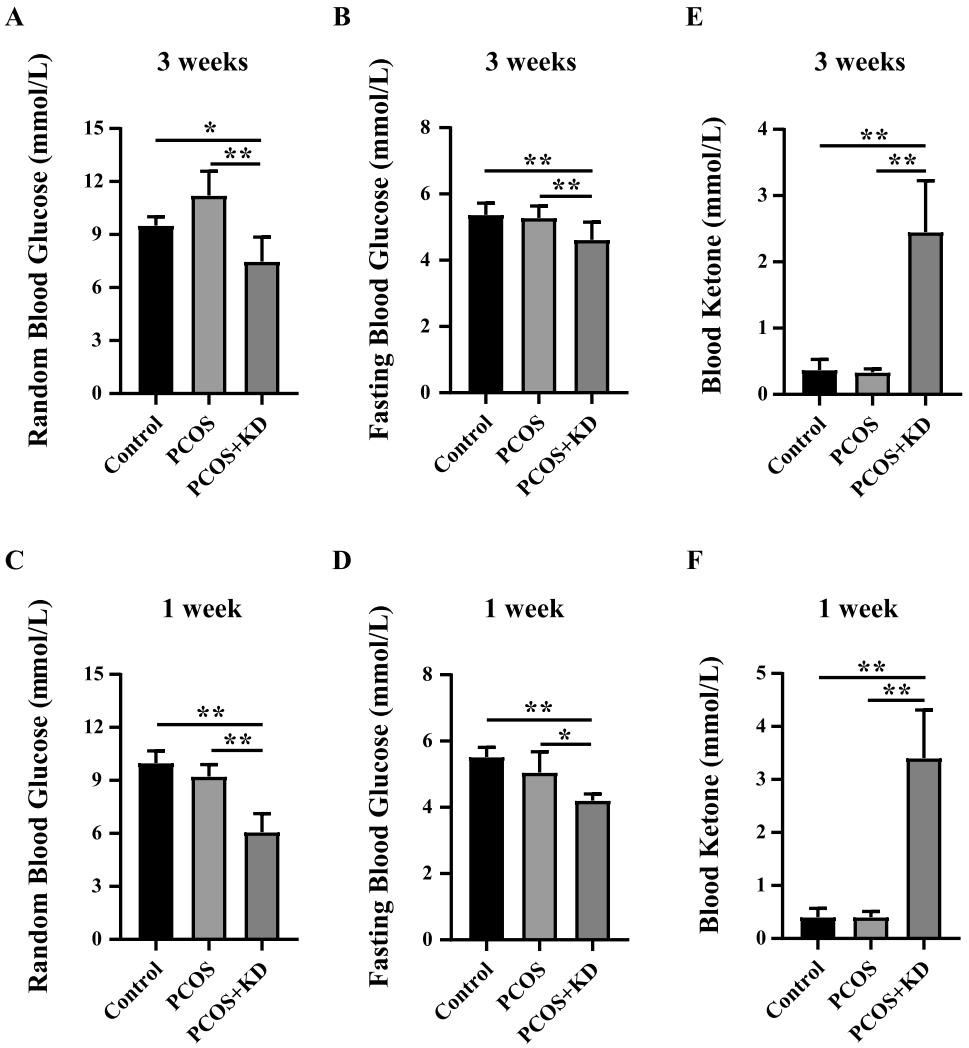

Figure 2. Effects of a KD feeding on blood glucose levels and ketone levels. (A) Random blood glucose of the mice treated with a control diet or KD for 3 weeks. (B) Fasting blood glucose of the mice treated with a control diet or KD for 3 weeks. (C) Random blood glucose of the mice treated with a control diet or KD for 1 week. (D) Fasting blood glucose of the mice treated with a control diet or KD for 1 week. (E) Ketone body of the mice treated with a control diet or KD for 3 weeks. (F) Ketone body of the mice treated with a control diet or KD for 1 week. Data are presented as mean ± SD. *, $P<0.05$, **, $P<0.01$, $n=6$ per group.

serum metabolomic assay to further investigate the effects of KD on the metabolites of DHEA mice. The results of volcano analysis showed great difference in metabolites between DHEA mice and DHEA+KD animals (Figure 6A). The differential metabolites included those related to lipid metabolism, such as β-hydroxybutyric acid (Figure 6B), butyrylcarnitine (Figure 6C), palmitoleic acid (Figure 6D), and oleic acid (Figure 6E), and those related to glucose metabolism, such as lactic acid (Figure 6F) and glyceraldehyde (Figure 6G), as well we other metabolites, such as orotic acid (Vitamin B13) (Figure 6H) and pantothenate (Vitamin B5) (Figure 6I).

KD reduced inflammation and apoptosis in ovarian granulosa cells

The proliferation and differentiation of granulosa cells are an important part of follicle development [12]. Chronic low-grade inflammation plays an important role in the pathogenesis of PCOS. Some studies have shown that serum and follicular fluid levels of inflammatory mediators are increased in women with PCOS [13, 14]. Since the KD treatment appeared to ameliorate ovarian function of some DHEA mice, we thus detected inflammation in the ovaries of these three groups of mice. RT-qPCR was performed to evaluate the mRNA expression of inflammatory factors interleukin-1β (IL-1β) and IL-6 in the ovaries of mice treated for 3 weeks. The results showed that KD treatment for 3 weeks decreased the mRNA expression of IL-1β and IL-6 in DHEA+KD mice compared with DHEA mice (Figure 7A).

Ketonemia is the most direct metabolic change and the most important indicator of the KD [15]. Among the three ketone bodies including acetoacetate, acetone, and BHB, BHB is the most important component, accounting for ~70% of the ketone bodies. Our results from in vivo experiments showed that serum BHB levels were significantly elevated after KD treatment. Therefore, BHB was used in in vitro experiments to simulate the effects of KD on the mice in vivo. As the most prominent effects of KD treatment seemed to be the improvement in ovarian function, KGN cells, a granulosa cell line, were thus used. Cells were pretreated with different concentrations of BHB for 6 h. Then, the cells were treated

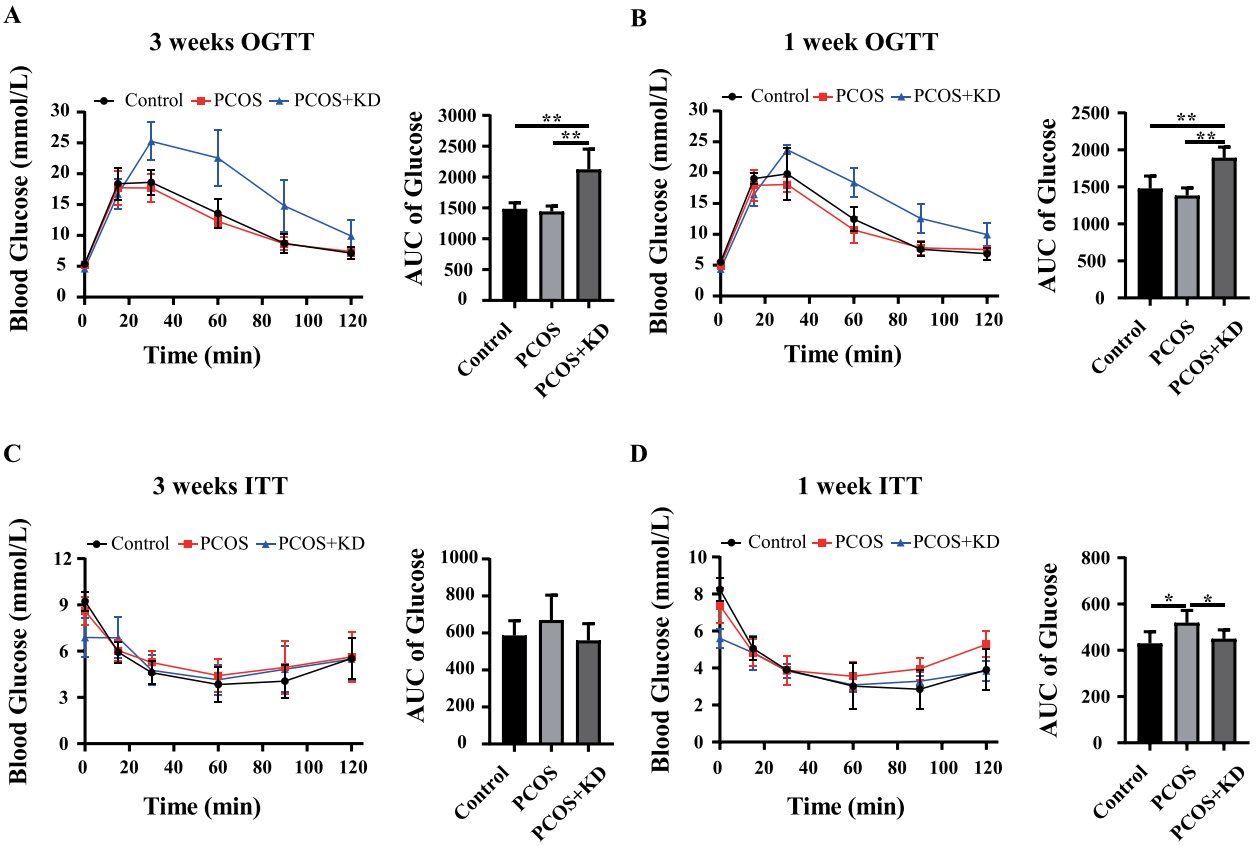

Figure 3. Effects of a KD feeding on glucose tolerance of the mice. (A) OGTT curve and AUC of OGTT of the mice treated with a control diet or KD for 3 weeks. (B) OGTT curve and AUC of OGTT of the mice treated with a control diet or KD for 1 week. (C) ITT curve and AUC of ITT of the mice treated with a control diet or KD for 3 weeks. (D) ITT curve and AUC of ITT of the mice treated with a control diet or KD for 1 week. Data are presented as mean ± SD. *, $P<0.05$, **, $P<0.01$, $n=6$ per group.

with the combination of BHB and DHEA (5×10^{-5} M) for 24 h. The concentration of 5×10^{-5} M DHEA was chosen based on our previous study (data not shown), which mimicked hyperandrogenism in DHEA-induced PCOS mice in vivo. After the treatments, cells were collected and the mRNA expression of IL-1β and IL-6 was detected. The results showed that treatment with DHEA significantly increased both IL-1β and IL-6 mRNA levels, indicating the presence of inflammation induced by DHEA treatment. There was no apparent difference in the IL-1β mRNA levels between the BHB + DHEA group and DHEA group. However, treatment of cells with BHB + DHEA decreased the IL-6 mRNA levels in a BHB concentration-dependent manner compared with DHEA group (Figure 7B). These results suggest that BHB treatment alleviated inflammation induced by DHEA in ovarian granulosa cells.

Cell apoptosis also plays an important role in the ovaries of PCOS. Results from TUNEL staining showed that the number of apoptotic granulosa cells was significantly decreased in the DHEA mice treated with KD for 1 or 3 weeks compared with DHEA mice fed normal diet (Figure 7C). We then treated KGN cells with DHEA (5×10^{-5} M) for 24 h, or pretreated with BHB for 6 h and then treated with the combination of DHEA and BHB for 24 h. MTT analysis showed the reduced cell viability in cells treated with DHEA compared with controls. The cell viability was increased in the DHEA+BHB group in a BHB concentration-dependent manner compared with the DHEA group (Figure 7D). We further investigated the effect of BHB on KGN cell apoptosis by detecting the protein levels of caspase 3 and cleaved-caspase 3. The cells were treated with DHEA (0, 5×10^{-5} M) or the combination of DHEA (5×10^{-5} M) and BHB (5 mM). Data from western blotting showed that the ratio of cleaved-caspase 3/caspase 3 values was significantly higher in the DHEA group than in controls, suggesting that DHEA induced apoptosis in KGN cells (Figure 7E). The treatment of KGN cells with the combination of DHEA and BHB (5 mM) reduced the ratio of cleaved-caspase 3/caspase 3 values compared with DHEA treatment alone. We also treated primary mGCs with DHEA (0, 5×10^{-5} M) and detected apoptosis with flow cytometry (FACS). Similar to KGN cells, DHEA significantly up-regulated the expression of cleavead Caspase-3 in primary mGCs, which was reduced by pre-treatment with BHB (Supplemental Figure S1). These results suggest that DHEA induced apoptosis of KGN cells and primary ganulosa cells, which can be reversed by BHB.

Discussion

The KD has been demonstrated to be highly effective in weight loss. In the clinic, the ketogenic dietary intervention has been used in obese or overweight women with PCOS and seems promising in improving both reproductive and metabolic disorders. The underlying mechanisms, however, have never been investigated. In the present study, the DHEA-induced PCOS mouse model was utilized and then treated

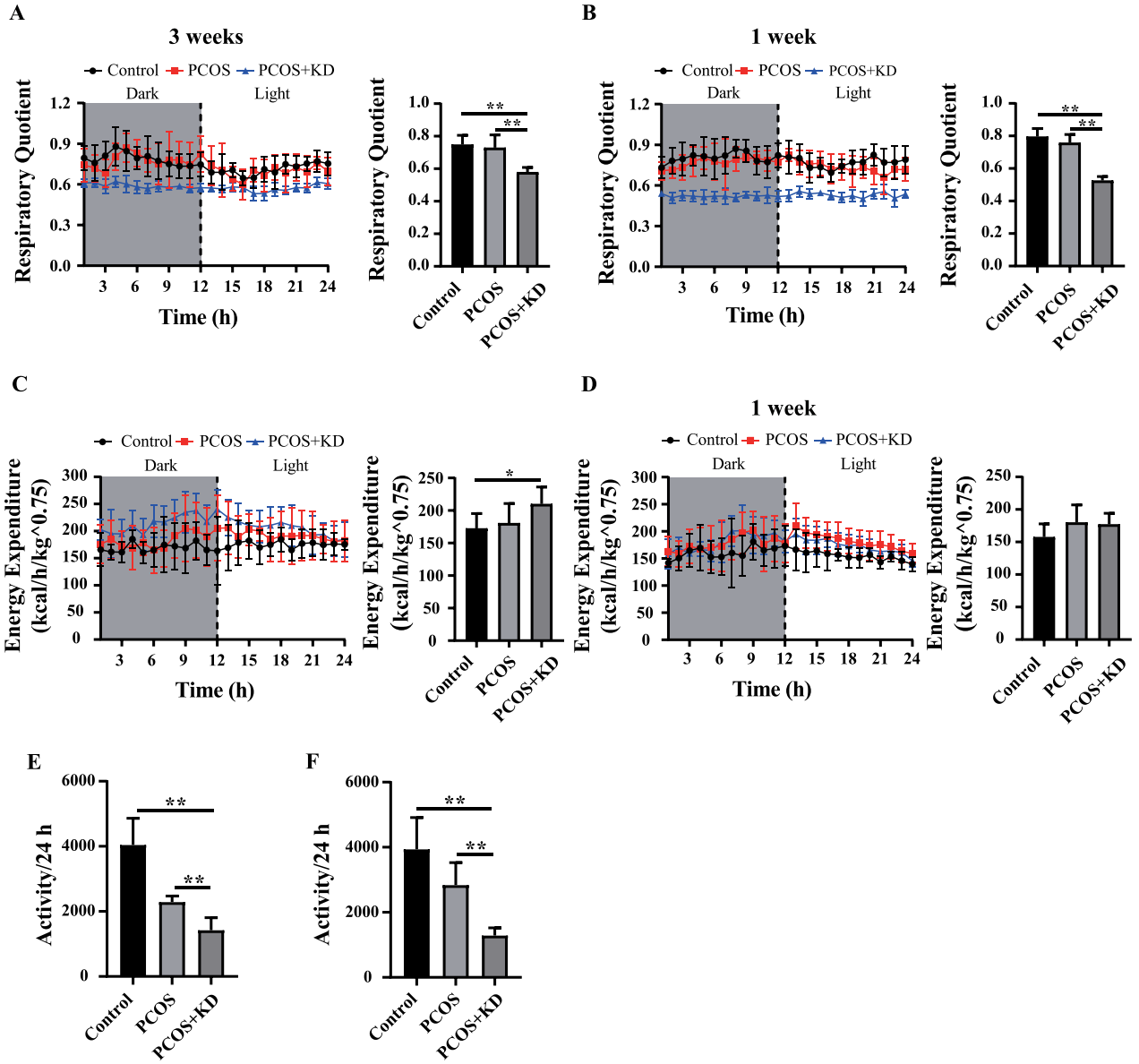

Figure 4. Effects of a KD feeding on RQ and EE. (A) RQ curve and average RQ of the mice treated with a control diet or KD for 3 weeks. (B) RQ curve and average RQ of the mice treated with a control diet or KD for 1 week. (C) EE curve and average EE of the mice treated with a control diet or KD for 3 weeks. (D) EE curve and average EE of the mice treated with a control diet or KD for 1 week. (E) The total activity of the mice for 24 h treated with a control diet or KD for 3 weeks. (F) The total activity of the mice for 24 h treated with a control diet or KD for 1 week. Data are presented as mean ± SD. *, $P<0.05$, **, $P<0.01$, $n=6$ per group.

with a KD for 1 and 3 weeks, respectively, to study the effects of KD on PCOS mice.

Consistent with other studies in weight loss by KD, KD treatment significantly reduced body weight and the intra-abdominal fat mass of DHEA mice. The reasons are complex. The DHEA+KD mice showed similar daily energy intake, higher EE, but less activity than DHEA mice. Moreno et al. [16] reported that more than 88% of patients with obesity lost more than 10% of their initial body weight after a 12-month period of the KD treatment, and the visceral fat mass was selectively reduced [17]. Another study also showed that weight loss by KD was primarily a reduction in body fat mass, particularly visceral fat mass [18]. According to previous studies, the possible mechanisms of weight loss by KD treatment include the reduced energy intake, increased energy consumption, and the promotion of lipid hydrolysis. The KD, as a high-fat and low-carbohydrate diet, supplies strong satiety. A study found that KD treatment can promote the secretion of leptin, suppress appetite, and reduce energy intake [19]. Control diet is high in carbohydrates (70% of calories from carbohydrates) and thus carbohydrates are the main nutrients for the oxidative energy supply of the mice. In contrast, KD is high in fat and low in carbohydrates. It caused the animals to use fat as their main energy source. KD leads to a switch of primary fuel from carbohydrate to lipid, which reduces the adipogenesis and promotes hydrolysis of fat to achieve the effect of weight loss. In our study, it seems possible that weight loss of DHEA mice by KD treatment was caused by the increased energy consumption due to the diet itself rather than changes in activity.

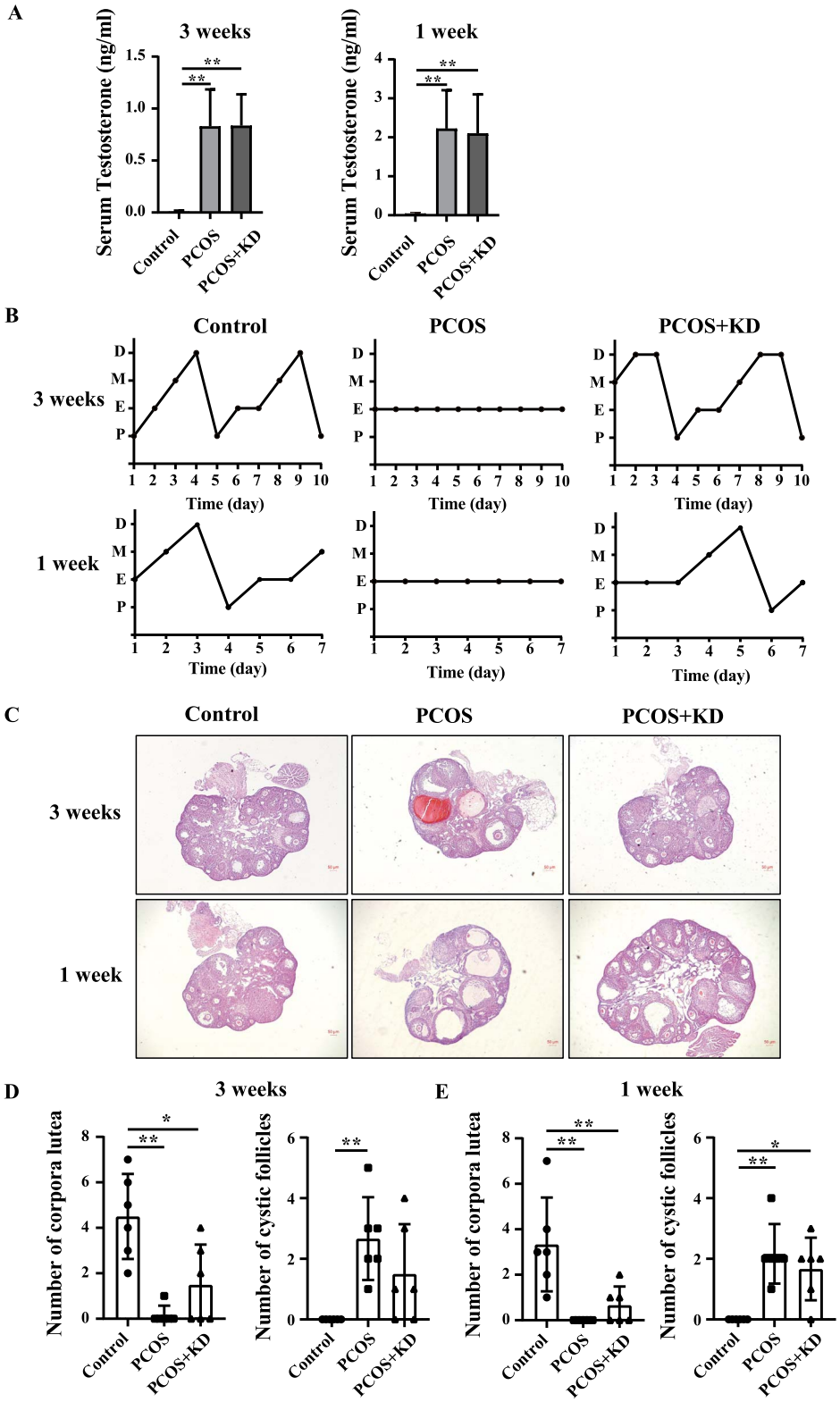

Figure 5. KD improves the ovarian function in DHEA mice. (A) Serum testosterone level of the mice treated with a control diet or KD for 1 or 3 weeks, respectively. (B) Representative estrous cycle of one mouse from each group. D, diestrus; M, metestrus; E, estrus; P, proestrus. (C) Representative H&E staining of ovarian sections of one mouse from each group. Micrographs were taken at magnifications ×40, bars = 50 μm. (D) The number of corpora lutea and cystic follicles of the mice treated with a control diet or KD for 3 weeks. (E) The number of corpora lutea and cystic follicles of the mice treated with a control diet or KD for 1 week. Data are presented as mean ± SD. *, $P<0.05$, **, $P<0.01$, $n=6$ per group.

Table 2. Statistics of estrous cycle in the three groups of mice.

	treatments for 3 weeks (n1/n2)	treatments for 1 week (n1/n2)
Control	6/6	6/6
PCOS	0/6	0/6
PCOS+KD	3/6	2/6

n1: The number of mice with normal ovarian morphology; n2: The total number of mice. $n = 6$ per group.

An initial case–control study showed that with 12-month ketogenic dietary intervention, the fasting blood glucose was significantly decreased and insulin sensitivity was alleviated in PCOS patients with obesity [20]. However, other study in C57BL/6 J mice found that after 12-week treatment of a KD, fasting blood glucose and insulin levels remained normal, while glucose tolerance of the mice was impaired [21]. In our study, we found the significantly reduced random and fasting blood glucose levels in DHEA treated with the KD for 1 or 3 weeks. Glucose tolerance was impaired in DHEA+KD mice treated for both 1 or 3 weeks. In contrast, insulin tolerance was improved in DHEA+KD mice treated for 1 week, but not for 3 weeks. These data suggest that the ketogenic dietary intervention was helpful to improving glycemic control and insulin sensitivity. The inconsistency in effects of KD on glucose tolerance between human and mouse studies is possibly due to the different components of KD, feeding term, and so on. Further research is warranted in the future.

A preliminary study about KD intervention in PCOS dated back to 2005. In this study, it was demonstrated that body weight, serum fasting insulin, serum free testosterone, and the ratios of luteinizing hormone (LH)/follicle-stimulating hormone (FSH) were significantly decreased and the fertility was improved after 24 weeks of KD treatment [9]. In our study, serum testosterone levels were not reduced either in 1- or 3-week treatment group. Human menstrual cycle contains three phases: menstruation, proliferative phase, and secretory phase. The human menstrual cycle enables ovarian development of one pre-ovulatory follicle and mid-cycle ovulation of a single oocyte at ~28-day intervals. However, women with PCOS often have irregular or absent menses and infrequent or absent ovulation [9]. In contrast, the estrous cycle of the mice can be divided into four stages: proestrus, estrus, metestrus, and diestrus. The mouse estrous cycle enables ovarian development of multiple dominant follicles and estrous cycle onset ovulation of multiple oocytes at 4- to 6-day intervals. PCOS mice showed disrupted estrous cycles, stagnating in estrus. In PCOS mouse model, KD treatment seems to improve ovarian function in some DHEA mice. To reveal the underlying mechanisms, we performed nontargeted metabolomics and in vitro experiments.

Data from nontargeted metabolomics showed significant changes in some metabolites. Butyryl carnitine, one of the significant indicators of abnormal lipid and energy metabolism [22], was significantly decreased in DHEA+KD mice, indicating that KD changed energy metabolism in these mice. A study showed that palmitic acid-induced IR by increasing the synthesis of deleterious complex lipids, impairing the function of cellular organelles, and receptor-mediated inflammation [23]. Interestingly, oleic acid can rescue palmitoleic acid-induced apoptosis and inflammation by promoting palmitoleic acid incorporation into triglyceride [23, 24]. The palmitic acid levels of the DHEA+KD mice were decreased and the oleic acid levels were increased, suggesting that KD treatment had a protective effect on DHEA mice. Additionally, several other studies have shown the critical role of oleic acid in counteracting the detrimental effects of saturated fatty acids and in paracrine support of oocyte development via mechanisms involving metabolic partitioning of fatty acids, change in the membrane structural organization, attenuation of oxidative stress, and regulation of intracellular signal pathway [25, 26]. Metabolite lactic acid has always been regarded as a metabolic by-product rather than a bioactive molecule, but it was discovered that lactic acid can be used as a signal molecule and has novel signal transduction functions both intracellularly and extracellularly, which can regulate key functions in the immune system [27]. The lactic acid levels of the DHEA and DHEA+KD mice were increased compared with Control mice, but there was no significant difference between DHEA and DHEA+KD animals. Profound fatty liver can be induced in certain vertebrates by the feeding of orotic acid [28–30]. However, there were no studies to report the effects of orotic acid on the liver of the mice. Interestingly, our results showed that the orotic acid levels of the DHEA mice increased compared with the Control mice. After KD treatment, the orotic acid levels returned to normal in the DHEA+KD mice. Pantothenate is necessary for steroid synthesis and exhibits antioxidant effects during inflammation [31]. The pantothenate levels of the DHEA+KD mice returned to normal levels compared with the DHEA mice, indicating a potential anti-inflammatory role of KD.

Ketone bodies are the intermediate products produced by oxidation of fat. BHB is the most important component of ketone bodies. Nontargeted metabolomics analysis showed the up-regulated serum BHB levels in DHEA+KD mice treated for 3 weeks, which was consistent with data of blood ketone level measurement. Serum pantothenate levels were significantly decreased in DHEA mice compared with controls but were markedly higher in DHEA+KD mice than in DHEA mice. Pantothenate is necessary for steroids synthesis and exhibits antioxidant effects during inflammation [31]. We therefore hypothesized that KD treatment may reverse ovarian dysfunction in PCOS mice by exerting an anti-inflammatory role.

Chronic low-level inflammation plays an important role in PCOS. Serum levels of inflammatory factors, such as TNFα, IL-6, and CRP, were significantly increased in patients with PCOS [32, 33]. The number of macrophages and inflammatory factors was significantly increased in the ovaries of women [34, 35] and PCOS mice [1] as well. Additionally, excess androgen can activate the ovarian NLRP3 inflammasome through TLR4. Then, the activation of the NLRP3 inflammasome led to the activation of caspase-1 and promoted the expression of inflammatory factors [33, 36]. In neurons, it was shown that BHB inhibited the NLRP3 inflammasome by inhibiting K^+ efflux and blocking ASC oligomerization and speckle formation [31], whether BHB plays an anti-inflammatory role in ovarian granulosa cells under the

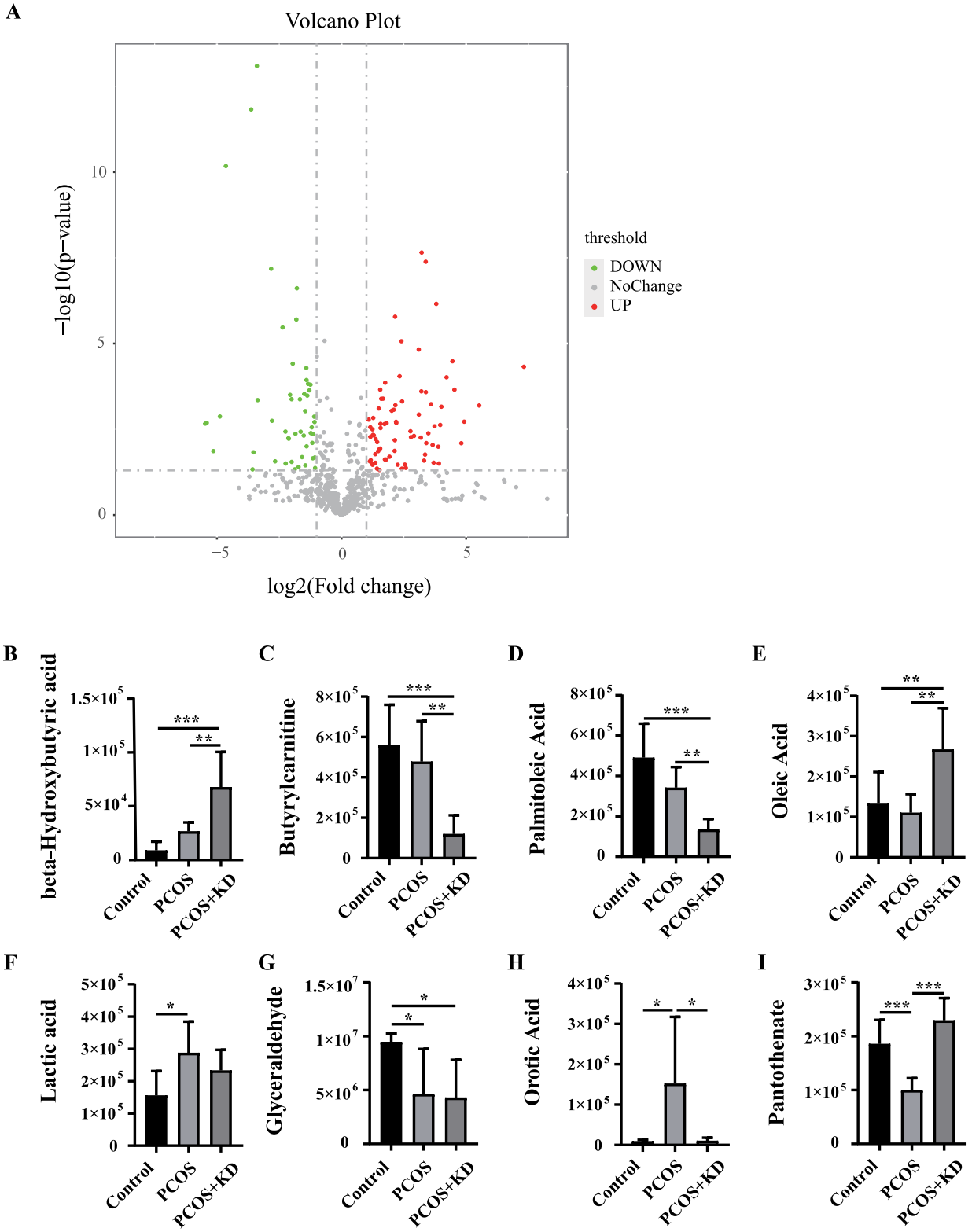

Figure 6. Results of serum nontargeted metabolomic analysis. (A) Volcano analysis of PCOS and PCOS+KD group mice treated with a control diet or KD for 3 weeks. (B–I) Significantly differential metabolites of the mice treated with a control diet or KD for 3 weeks: (B) β-hydroxybutyric acid, (C) Butyrylcarnitine, (D) Palmitoleic acid, (E) Oleic acid, (F) Lactic acid, (G) Glyceraldehyde, (H) Orotic acid, and (I) Pantothenate. Data are presented as mean ± SD. *, $P<0.05$, **, $P<0.01$, ***, $P<0.001$, $n=8$ per group.

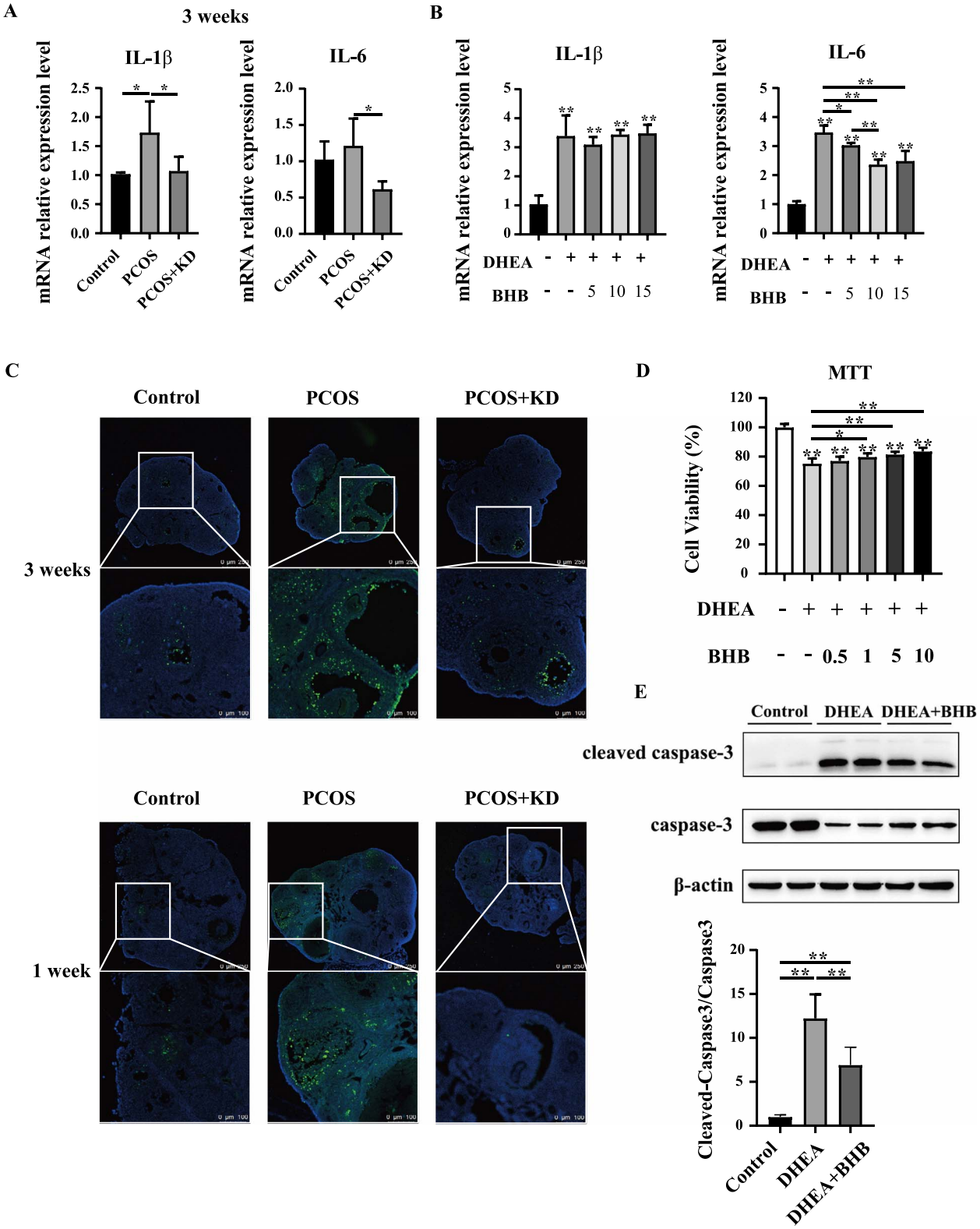

Figure 7. KD alleviates inflammation and cell apoptosis in ovarian granulosa cells. (A) The mRNA expression levels of IL-1β and IL-6 in the ovaries of the mice treated with a control diet or KD for 3 weeks. $n=6$ per group. (B) The mRNA expression levels of IL-1β and IL-6 in KGN cells treated with DHEA (0, 5×10^{-5} M) or the combination of DHEA (5×10^{-5} M) and BHB at different concentrations. (C) Representative photomicrographs of TUNEL staining in the ovaries. $n=5$ per group. (D) Cell viability measured by MTT. KGN cells were treated with DHEA (0, 5×10^{-5} M) or the combination of DHEA (5×10^{-5} M) and BHB at different concentrations. Then, cell viability was measured. (E) Protein levels of caspase 3 and cleaved-caspase 3 in KGN cells treated with DHEA (0, 5×10^{-5} M) or the combination of DHEA (5×10^{-5} M) and BHB (5 mM). Marks labeled directly on the panels represented comparisons with the controls. Data are presented as mean ± SD. *, $P<0.05$, **, $P<0.01$. The assay was performed in triplicate and repeated 3 times.

circumstance of PCOS is unknown. In the present study, for the first time, we showed that KD treatment exhibited anti-inflammatory effects in ovaries of PCOS mice. Data from in vitro experiments further demonstrated that DHEA induced levels of inflammatory factors IL-1β and IL-6 in KGN cells. BHB treatment decreased the DHEA-induced IL-6 levels, but not IL-1β. The reason is still unknown.

Cell apoptosis also plays an important role in ovarian dysfunction in PCOS [37, 38]. Results of TUNEL staining showed the increased apoptotic granulosa cells in the ovaries of DHEA mice but decreased in the DHEA+KD mice. Data from in vitro experiment showed the increased ratio of cleaved caspase-3/caspase-3 in cells treated with DHEA, indicating the elevated cell apoptosis by DHEA treatment. As expected, BHB treatment reduced the ratio of cleaved caspase-3/caspase-3, suggesting the anti-apoptosis effects of BHB in KGN cells.

Taken together, KD treatment might improve ovarian function in PCOS mice by inhibiting inflammation and cell apoptosis in ovarian granulosa cells.

In summary, our data support the role of KD intervention in weight loss, reducing blood glucose, and improving ovarian functions in PCOS mice. For the first time, we also showed the possible mechanisms by which KD improved ovarian functions by inhibiting inflammation and cell apoptosis in ovarian granulosa cells in PCOS.

There are some limitations of this study. Due to the shortage of serum samples, serum levels of LH, FSH, and estradiol were not measured. In addition, the mechanisms should to be further explored in the future studies.

Supplementary material

Supplementary material is available at *BIOLRE* online.

Data availability

The data underlying this article will be shared on reasonable request to the corresponding author.

Authors' contributions

S.L., Q.Y. and H.W. performed the experiments. S.L., Q.Y., H.W., and C.S. analyzed the data. J.K., W.B., and X.L. conceived the experimental designs. S.L., Q.Y., and J.K. wrote the manuscript.

Acknowledgment

We thank Jiye Hou at Shanghai Bioprofile Technology Company Ltd. for his technical support in Metabolomics.

Conflict of interest

No conflict of interest exists.

References

1. Shen HR, Xu X, Li XL. Berberine exerts a protective effect on rats with polycystic ovary syndrome by inhibiting the inflammatory response and cell apoptosis. *Reprod Biol Endocrinol* 2021; **19**: 3–14.
2. Wang J, Wu D, Guo H, Li M. Hyperandrogenemia and insulin resistance: the chief culprit of polycystic ovary syndrome. *Life Sci* 2019; **236**:116940.
3. Li J, Bai WP, Jiang B, Bai LR, Gu B, Yan SX, Li FY, Huang B. Ketogenic diet in women with polycystic ovary syndrome and liver dysfunction who are obese: a randomized, open-label, parallel-group, controlled pilot trial. *J Obstet Gynaecol Res* 2021; **47**: 1145–1152.
4. Neves LPP, Marcondes RR, Maffazioli GN, Simoes RS, Maciel GAR, Soares JM Jr, Baracat EC. Nutritional and dietary aspects in polycystic ovary syndrome: insights into the biology of nutritional interventions. *Gynecol Endocrinol* 2020; **36**:1047–1050.
5. Lai H, Jia X, Yu Q, Zhang C, Qiao J, Guan Y, Kang J. High-fat diet induces significant metabolic disorders in a mouse model of polycystic ovary syndrome. *Biol Reprod* 2014; **91**:127–138.
6. Zhu H, Bi D, Zhang Y, Kong C, Du J, Wu X, Wei Q, Qin H. Ketogenic diet for human diseases: the underlying mechanisms and potential for clinical implementations. *Signal Transduct Target Ther* 2022; **7**:11–32.
7. Augustin K, Khabbush A, Williams S, Eaton S, Orford M, Cross JH, Heales SJR, Walker MC, Williams RSB. Mechanisms of action for the medium-chain triglyceride ketogenic diet in neurological and metabolic disorders. *The Lancet Neurology* 2018; **17**:84–93.
8. Phillips MCL, Deprez LM, Mortimer GMN, Murtagh DKJ, McCoy S, Mylchreest R, Gilbertson LJ, Clark KM, Simpson PV, McManus EJ, Oh JE, Yadavaraj S *et al.* Randomized crossover trial of a modified ketogenic diet in Alzheimer's disease. *Alzheimers Res Ther* 2021; **13**:51–63.
9. Mavropoulos JC, Yancy WS, Hepburn J, Westman EC. The effects of a low-carbohydrate, ketogenic diet on the polycystic ovary syndrome: a pilot study. *Nutr Metab (Lond)* 2005; **2**:35–40.
10. Zhu M, Shen Q, Li X, Kang J. Removal of peri-ovarian adipose tissue affects follicular development and lipid metabolismdagger. *Biol Reprod* 2020; **103**:1199–1208.
11. Worku T, Wang K, Ayers D, Wu D, Ur Rehman Z, Zhou H, Yang L. Regulatory roles of ephrinA5 and its novel signaling pathway in mouse primary granulosa cell apoptosis and proliferation. *Cell Cycle* 2018; **17**:892–902.
12. Monte APO, Bezerra MES, Menezes VG, Gouveia BB, Barberino RS, Lins T, Barros VRP, Santos JMS, Donfack NJ, Matos MHT. Involvement of phosphorylated Akt and FOXO3a in the effects of growth and differentiation Factor-9 (GDF-9) on inhibition of follicular apoptosis and induction of granulosa cell proliferation after in vitro culture of sheep ovarian tissue. *Reprod Sci* 2021; **28**: 2174–2185.
13. Khichar A, Gupta S, Mishra S, Meena M. Assessment of inflammatory markers in women with PCOS and their correlation with insulin resistance. *Clin Lab* 2021; **67**(11):1433–1445.
14. Abraham Gnanadass S, Divakar Prabhu Y, Valsala GA. Association of metabolic and inflammatory markers with polycystic ovarian syndrome (PCOS): an update. *Arch Gynecol Obstet* 2021; **303**:631–643.
15. Dowis K, Banga S. The potential health benefits of the ketogenic diet: a narrative review. *Nutrients* 2021; **13**:1654–1683.
16. Moreno B, Bellido D, Sajoux I, Goday A, Saavedra D, Crujeiras AB, Casanueva FF. Comparison of a very low-calorie-ketogenic diet with a standard low-calorie diet in the treatment of obesity. *Endocrine* 2014; **47**:793–805.
17. Moreno B, Crujeiras AB, Bellido D, Sajoux I, Casanueva FF. Obesity treatment by very low-calorie-ketogenic diet at two years: reduction in visceral fat and on the burden of disease. *Endocrine* 2016; **54**:681–690.
18. Gomez-Arbelaez D, Bellido D, Castro AI, Ordonez-Mayan L, Carreira J, Galban C, Martinez-Olmos MA, Crujeiras AB, Sajoux I, Casanueva FF. Body composition changes after very-low-calorie ketogenic diet in obesity evaluated by 3 standardized methods. *J Clin Endocrinol Metab* 2017; **102**:488–498.
19. Roekenes J, Martins C. Ketogenic diets and appetite regulation. *Curr Opin Clin Nutr Metab Care* 2021; **24**:359–363.

20. Paoli A, Mancin L, Giacona MC, Bianco A, Caprio M. Effects of a ketogenic diet in overweight women with polycystic ovary syndrome. *J Transl Med* 2020; **18**:104–115.
21. Garbow JR, Doherty JM, Schugar RC, Travers S, Weber ML, Wentz AE, Ezenwajiaku N, Cotter DG, Brunt EM, Crawford PA. Hepatic steatosis, inflammation, and ER stress in mice maintained long term on a very low-carbohydrate ketogenic diet. *Am J Physiol Gastrointest Liver Physiol* 2011; **300**: G956–G967.
22. Cheng ML, Wang CH, Shiao MS, Liu MH, Huang YY, Huang CY, Mao CT, Lin JF, Ho HY, Yang NI. Metabolic disturbances identified in plasma are associated with outcomes in patients with heart failure: diagnostic and prognostic value of metabolomics. *J Am Coll Cardiol* 2015; **65**:1509–1520.
23. Palomer X, Pizarro-Delgado J, Barroso E, Vazquez-Carrera M. Palmitic and oleic acid: the yin and Yang of fatty acids in type 2 diabetes mellitus. *Trends Endocrinol Metab* 2018; **29**: 178–190.
24. Listenberger LL, Han X, Lewis SE, Cases S, Farese RV Jr, Ory DS, Schaffer JE. Triglyceride accumulation protects against fatty acid-induced lipotoxicity. *Proc Natl Acad Sci U S A* 2003; **100**: 3077–3082.
25. Fayezi S, Leroy J, Ghaffari Novin M, Darabi M. Oleic acid in the modulation of oocyte and preimplantation embryo development. *Zygote* 2018; **26**:1–13.
26. Renaville B, Bacciu N, Comin A, Motta M, Poli I, Vanini G, Prandi A. Plasma and follicular fluid fatty acid profiles in dairy cows. *Reprod Domest Anim* 2010; **45**:118–121.
27. Zhou HC, Xin-Yan Y, Yu WW, Liang XQ, Du XY, Liu ZC, Long JP, Zhao GH, Liu HB. Lactic acid in macrophage polarization: the significant role in inflammation and cancer. *Int Rev Immunol* 2022; **41**:4–18.
28. Jung EJ, Kwon SW, Jung BH, Oh SH, Lee BH. Role of the AMPK/SREBP-1 pathway in the development of orotic acid-induced fatty liver. *J Lipid Res* 2011; **52**:1617–1625.
29. Durschlag RP, Robinson JL. Orotic acid-induced metabolic changes in the rat. *J Nutr* 1980; **110**:816–821.
30. Jiang Z, Kimura Y, Shirouchi B, Tanaka Y, Tsai WT, Yuan X, Sato M. Dietary egg white protein hydrolysate improves orotic acid-induced fatty liver in rats by promoting hepatic phospholipid synthesis and microsomal triglyceride transfer protein expression. *J Nutr Biochem* 2021; **98**:108820.
31. Youm YH, Nguyen KY, Grant RW, Goldberg EL, Bodogai M, Kim D, D'Agostino D, Planavsky N, Lupfer C, Kanneganti TD, Kang S, Horvath TL *et al*. The ketone metabolite beta-hydroxybutyrate blocks NLRP3 inflammasome-mediated inflammatory disease. *Nat Med* 2015; **21**:263–269.
32. Dhindsa G, Bhatia R, Dhindsa M, Bhatia V. Insulin resistance, insulin sensitization and inflammation in polycystic ovarian syndrome. *J Postgrad Med* 2004; **50**:140–144.
33. Wang D, Weng Y, Zhang Y, Wang R, Wang T, Zhou J, Shen S, Wang H, Wang Y. Exposure to hyperandrogen drives ovarian dysfunction and fibrosis by activating the NLRP3 inflammasome in mice. *Sci Total Environ* 2020; **745**:141049.
34. Rudnicka E, Kunicki M, Suchta K, Machura P, Grymowicz M, Smolarczyk R. Inflammatory markers in women with polycystic ovary syndrome. *Biomed Res Int* 2020; **2020**:4092470.
35. Xiong YL, Liang XY, Yang X, Li Y, Wei LN. Low-grade chronic inflammation in the peripheral blood and ovaries of women with polycystic ovarian syndrome. *Eur J Obstet Gynecol Reprod Biol* 2011; **159**:148–150.
36. Xu B, Zhang YW, Tong XH, Liu YS. Characterization of microRNA profile in human cumulus granulosa cells: identification of microRNAs that regulate notch signaling and are associated with PCOS. *Mol Cell Endocrinol* 2015; **404**:26–36.
37. Salehi E, Aflatoonian R, Moeini A, Yamini N, Asadi E, Khosravizadeh Z, Tarzjani MD, Harat ZN, Abolhassani F. Apoptotic biomarkers in cumulus cells in relation to embryo quality in polycystic ovary syndrome. *Arch Gynecol Obstet* 2017; **296**: 1219–1227.
38. Uyanikoglu H, Sabuncu T, Dursun H, Sezen H, Aksoy N. Circulating levels of apoptotic markers and oxidative stress parameters in women with polycystic ovary syndrome: a case-controlled descriptive study. *Biomarkers* 2017; **22**:643–647.